

UNCLASSIFIED

PRODUCTION OF ELECT  
AUG 82 J M HERBEL  
TR-0082(2930-01)-2

F04701-81-C-0082

NL

1 of  
ADA  
10539

END

DATE  
FILMED

10

DTIC



AD A119539

# Production of Electronically Excited Bi( $^2D_{3/2}$ )

J. M. HERBELIN, R. R. GIEDT, and H. A. BIXLER  
Aerophysics Laboratory  
Laboratory Operations  
The Aerospace Corporation  
El Segundo, Calif. 90245

16 August 1982

DTIC FILE COPY

APPROVED FOR PUBLIC RELEASE;  
DISTRIBUTION UNLIMITED

DTIC  
ELECTE  
SEP 24 1982  
S H D

Prepared for  
SPACE DIVISION  
AIR FORCE SYSTEMS COMMAND  
Los Angeles Air Force Station  
P.O. Box 92960, Worldway Postal Center  
Los Angeles, Calif. 90009

82 00 24 072

This report was submitted by The Aerospace Corporation, El Segundo, CA 90245, under Contract No. F04701-81-C-0082 with the Space Division, Deputy for Technology, P.O. Box 92960, Worldway Postal Center, Los Angeles, CA 90009. It was reviewed and approved for The Aerospace Corporation by W. P. Thompson, Director, Aerophysics Laboratory. Lt Efren F. Fornoles, SD/YLXT, was the project officer for the Mission-Oriented Investigation and Experimentation (MOIE) Program.

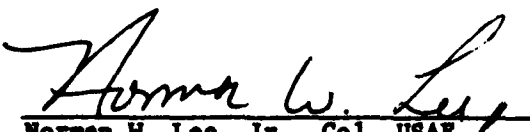
This report has been reviewed by the Public Affairs Office (PAS) and is releasable to the National Technical Information Service (NTIS). At NTIS, it will be available to the general public, including foreign nations.

This technical report has been reviewed and is approved for publication. Publication of this report does not constitute Air Force approval of the report's findings or conclusions. It is published only for the exchange and stimulation of ideas.

  
Efren V. Fornoles, 1st Lt, USAF  
Project Officer

  
Jimmie H. Butler, Colonel, USAF  
Director of Space Systems Technology

FOR THE COMMANDER

  
Norman W. Lee, Jr., Col, USAF  
Deputy for Technology

UNCLASSIFIED

SECURITY CLASSIFICATION OF THIS PAGE (When Data Entered)

REPORT DOCUMENTATION PAGE		READ INSTRUCTIONS BEFORE COMPLETING FORM
1. REPORT NUMBER SD-TR-82-57	2. GOVT ACCESSION NO. AD-A119539	3. RECIPIENT'S CATALOG NUMBER
4. TITLE (and Subtitle)  PRODUCTION OF ELECTRONICALLY EXCITED $\text{Bi}(^2\text{D}_{3/2})$		5. TYPE OF REPORT & PERIOD COVERED
7. AUTHOR(s)  John M. Herbelin, Robert Giedt, and Henry A. Bixler		6. PERFORMING ORG. REPORT NUMBER TR-0082(2930-01)-2
9. PERFORMING ORGANIZATION NAME AND ADDRESS  The Aerospace Corporation El Segundo, Calif. 90245		8. CONTRACT OR GRANT NUMBER(s)  F04701-81-C-0082
11. CONTROLLING OFFICE NAME AND ADDRESS Space Division Air Force Systems Command Los Angeles, Calif. 90009		10. PROGRAM ELEMENT, PROJECT, TASK AREA & WORK UNIT NUMBERS
14. MONITORING AGENCY NAME & ADDRESS (if different from Controlling Office)		12. REPORT DATE 16 August 1982
		13. NUMBER OF PAGES 23
		15. SECURITY CLASS. (of this report)  Unclassified
		15a. DECLASSIFICATION/DOWNGRADING SCHEDULE
16. DISTRIBUTION STATEMENT (of this Report)  Approved for public release; distribution unlimited		
17. DISTRIBUTION STATEMENT (of the abstract entered in Block 20, if different from Report)		
18. SUPPLEMENTARY NOTES  (a single Delta)		
19. KEY WORDS (Continue on reverse side if necessary and identify by block number)  Chemical laser Chemical transfer laser Supersonic diffusion laser Reactive flow  (a) (b) (c) (d) (e) (f) (g) (h) (i) (j) (k) (l) (m) (n) (o) (p) (q) (r) (s) (t) (u) (v) (w) (x) (y) (z)		
20. ABSTRACT (Continue on reverse side if necessary and identify by block number) Emission signals at 8758 Å were observed when bismuth atom vapor was introduced into a supersonic flow of electronically excited nitrogen fluoride, $\text{NF}(^2\text{A})$ . A correlation of thermal and pressure data with the appearance of the chemiluminescence, along with a computer analysis of the IRTV observations at two wavelengths, is presented. On the basis of an analysis of these data, it is concluded that the observed emission results from the production of an excited-state bismuth atom density, $\text{Bi}(^2\text{D}_{3/2})$ , on the order of $> 10^{13}$ atoms $\text{cm}^{-3}$ by collisional transfer with $\text{NF}(^2\text{A})$ .		

DD FORM 1473  
(IFACSIMILE)

UNCLASSIFIED

SECURITY CLASSIFICATION OF THIS PAGE (When Data Entered)

**UNCLASSIFIED**

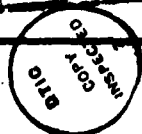
**SECURITY CLASSIFICATION OF THIS PAGE(When Data Entered)**

**19. KEY WORDS (Continued)**

Metal atom injection  
Flow visualization  
Infrared television  
Nitrogen fluoride  
Bismuth  
Seeding

**20. ABSTRACT (Continued)**

Accession	✓
NTIS	
DTIC	
Unann.	
Just.	
By	
Distrib.	
Avail.	With Copies
Dist	
A	



**UNCLASSIFIED**

**SECURITY CLASSIFICATION OF THIS PAGE(When Data Entered)**

#### ACKNOWLEDGMENTS

The authors are deeply indebted to R. E. Cook for his assistance in performing the flow experiments and in constructing the metal injectors. The infrared television work was performed by the skillful O. L. Gibb under the supervision of E. F. Cross, and computer analysis of these data was the result of the very talented and hard-working C. I. Segal. The authors are also very grateful to M. A. Kwok for his many helpful suggestions.

This work was supported in part by the Air Force Weapons Laboratory under U.S. Air Force Space Division Contract (SD) F04701-81-C-0082.

## CONTENTS

ACKNOWLEDGMENTS.....	1
I. INTRODUCTION.....	5
II. EXPERIMENTAL.....	7
III. RESULTS AND DISCUSSION.....	15
REFERENCES.....	23

## FIGURES

1.	Schematic Drawing of the Supersonic Flow Facility.....	8
2.	Rise in Injector Temperature as a Function of Current Passed through Heater.....	10
3.	Rise in Injector Temperature as a Function of Arc Current Used to Heat Plenum Gases.....	11
4.	Computed Line Spectra of Bismuth and NF Emissions, with Transmission Curves of the Two Narrow-Band Filters.....	12
5.	Schematic of the Physical Arrangement of the Two Infrared-Sensitive Video Cameras with Respect to the Beta Flow Test Chamber.....	13
6.	Static Pressure of the Supersonic Flow and Computed Bismuth Atom Vapor Pressure inside Injector.....	16
7.	Relationship of Injector Temperature to Increase in Arc Current with Time.....	17
8.	Two-Dimensional Representations of the Emission Observed through the 8758-Å Filter after Being Digitized by the Quantex.....	19
9.	Vertical Scans for Upstream and Downstream Cross Scale Positions Indicated in Fig. 8.....	20
10.	Horizontal Scans for Upstream and Downstream Cross Scale Positions Indicated in Fig. 8.....	21



## I. INTRODUCTION

The objective of this work was to explore the possibility of producing large densities of electronically excited bismuth atoms,  $\text{Bi}(^2\text{D}_{3/2})$ , by collisional transfer with electronically excited nitrogen fluoride radicals,  $\text{NF}(a^1\Delta)$ . Herbelin and Cohen<sup>1,2</sup> have suggested that  $\text{NF}(a^1\Delta)$  can be efficiently produced by chemical reaction by a reaction channel that strongly favors this excited electronic state. Recent work by Cheah, Clyne, and Whitefield,<sup>3</sup> and also by Malins and Setser,<sup>4</sup> supports this conclusion. Herbelin, Spencer, and Kwok<sup>5</sup> have demonstrated that large concentrations of the electronically excited  $\text{NF}(a^1\Delta)$  could be produced in a sonic flow by means of this chemical reaction scheme. This scaling was repeated by Miller<sup>6</sup> in a combustor-driven flow facility and scaled to larger concentrations by Herbelin, et al.,<sup>7</sup> in a larger supersonic flow.

Capelle and Sutton<sup>8</sup> have shown that a resonant collisional transfer from  $\text{NF}(a^1\Delta)$  to  $\text{Bi}(^4\text{S}_{3/2})$  is extremely fast and efficient. This result, combined with the stimulated emission cross section of the  $\text{Bi}(^2\text{D}_{3/2}) - \text{Bi}(^4\text{S}_{3/2})$  transition at 8758 Å ( $\sigma \approx 7 \times 10^{-18} \text{ cm}^2$ ),<sup>9</sup> much larger than the  $\text{NF}(a^1\Delta) - \text{NF}(X^3\Sigma^-)$  transition at 8742 Å ( $\sigma \approx 2 \times 10^{-21} \text{ cm}^2$ ),<sup>4</sup> strongly suggests the possibility of a transfer laser system. (The  $\sigma$ 's are computed from the radiative lifetimes reported in cited references.) An important step in developing such a laser system would be to demonstrate the feasibility of introducing bismuth atoms into a flow containing a large density of  $\text{NF}(a^1\Delta)$ , in particular the large supersonic flow facility.

In this report we describe our observation of (8758 Å) chemiluminescence believed to be emitted by electronically excited bismuth atoms. The emission occurs when a heated injector containing bismuth is placed in a supersonic flow of electronically excited  $\text{NF}(a^1\Delta)$ . A correlation of thermal and pressure data with the appearance of the chemiluminescence, along with a computer analysis of the infrared video observations at two wavelengths, is presented. On the basis of the combined analysis of these data, we concluded that the

observed emission results from the production of an excited-state bismuth atom density,  $\text{Bi}(^2\text{D}_{3/2})$ , on the order of  $10^{13}$  atoms- $\text{cm}^{-3}$  by collisional transfer with  $\text{NF}(a^1\Delta)$ .

## II. EXPERIMENTAL

Figure 1 is a schematic drawing of the supersonic flow facility, henceforth referred to as the Beta Facility. The facility employs an arc-driven plenum ( $T \approx 1700$  K) to produce a flow of fluorine atoms, in the presence of a helium diluent, which is then expanded through a Mach 2.2 nozzle. At this point tetrafluorohydrazine,  $N_2F_4$ , is introduced through a wall injector consisting of two rows of alternating holes of 0.23-mm diameter spaced 0.64 mm apart. As a consequence of the partial stagnation, the static temperature of the flow was in the range of 900 K to 1150 K. This provides for the thermal dissociation of the  $N_2F_4$  into difluoroamine radicals,  $NF_2$ . A diffuser or spacer plate is used to extend this hot zone, which expands rapidly into the shroud section. The degree of expansion is adjustable by means of the steps or base relief, which can be varied by moving the shrouds up and down independently. For these experiments, and in order to accommodate the insertion of the metal-atom injector tube, the shrouds were placed in their full-open position, which corresponded to a separation of 12.5 mm at the hydrogen injectors. The two  $H_2$  injectors consisted of a row of 0.33-mm-diameter holes spaced at 1.27-mm intervals and were used to inject a 1:1 mixture of hydrogen and helium, the latter element being used to increase the jet penetration. Visible and infrared video pictures indicated that the two hydrogen gas streams coming from the opposite sides would meet at the center of the flow at approximately 0.25 in. downstream of the injector holes under all gas-flow conditions.

The Beta flow facility and flow conditions are described in detail elsewhere.<sup>7</sup> For our purposes here it should be sufficient to say that, with the recent report by Malins and Setser<sup>4</sup> concerning the radiative lifetime of  $NF(a^1\Delta)$ , we concluded that this flow utilized in excess of 50% of the limiting reagent species (F atoms) to produce densities of  $NF(a^1\Delta) = 6 \times 10^{15}$  molecules  $cm^{-3}$  over its flow width of 18 cm.

The metal-atom injector was located 12.7 mm downstream of the hydrogen injectors at approximately the point of peak  $NF(a^1\Delta)$  concentration. It consisted of a very simple design, a partially flattened No. 12 gauge stainless-

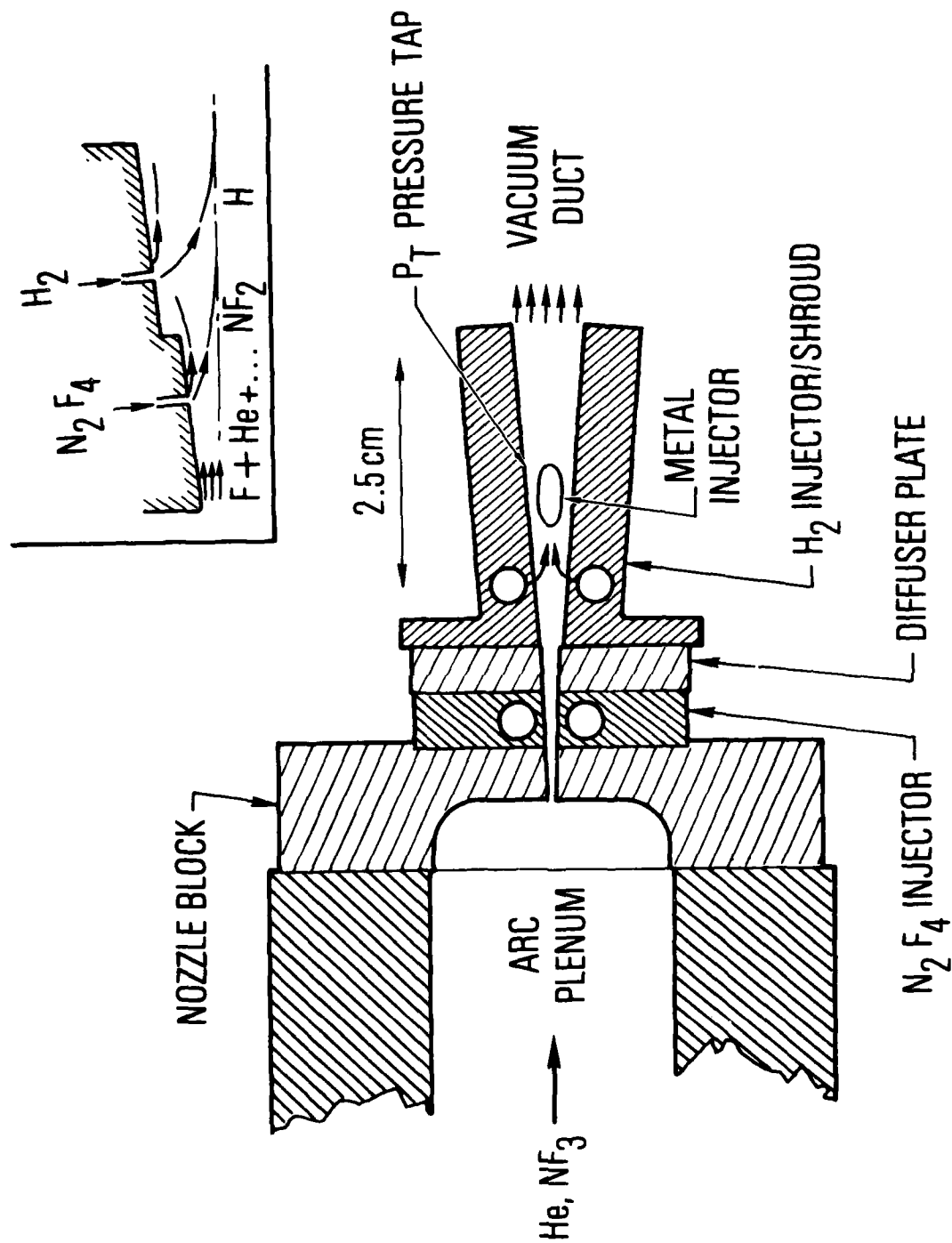


Fig. 1. Schematic Drawing of the Su-16 Vacuum Facility

steel tube. Holes of 4.57-mm diameter 12.7 mm apart were drilled in the top of this flattened tube. Bismuth, in the form of long strips ( $6.0 \times 3.0 \times 200$  mm) was inserted in the tube. A thermocouple was also inserted in the tube and its tip was positioned on the leading edge at the center of the injector. The tube was sealed at both ends to prevent the escape of bismuth liquid or vapor during the experiment.

The injector was attached directly to the Beta shrouds at one end by means of a mounting brace, and to a spring-loaded holder at the other. The spring-loaded mounting was necessary to accommodate the expansion of the stainless-steel tube during the heating. The injector could be heated by passing an electrical current through it (Fig. 2). However, it was discovered that the temperature rise resulting from the stagnation of the flow itself was sufficient to achieve the required elevated temperatures. In Fig. 3 we show the rise in the injector temperature, as measured by the thermocouple, as a function of the arc current used to heat the plenum gases. The two curves shown correspond to the cases of helium only and when all the gases are flowing.

To monitor and distinguish the bismuth atom chemiluminescence at 8758 Å from the  $\text{NF}(a^1\Delta)$  emission in the same region, we used a two-camera, two-wavelength diagnostic. The computed line spectra of the bismuth<sup>10,11</sup> and NF emissions,<sup>12</sup> along with the transmission curves of the two narrow-band filters used in these experiments, are shown in Fig. 4. Figure 5 shows a schematic of the physical arrangement of the two infrared-sensitive GBC-ITT video cameras (model CTC-5000) with respect to the Beta flow test chamber. The 50/50 pellicle affords each camera an identical field of vision to minimize any errors resulting from parallax.

The video information was stored on cassette tapes for subsequent analysis by means of a Quantex digitizer coupled with a PDP 11/10 computer.

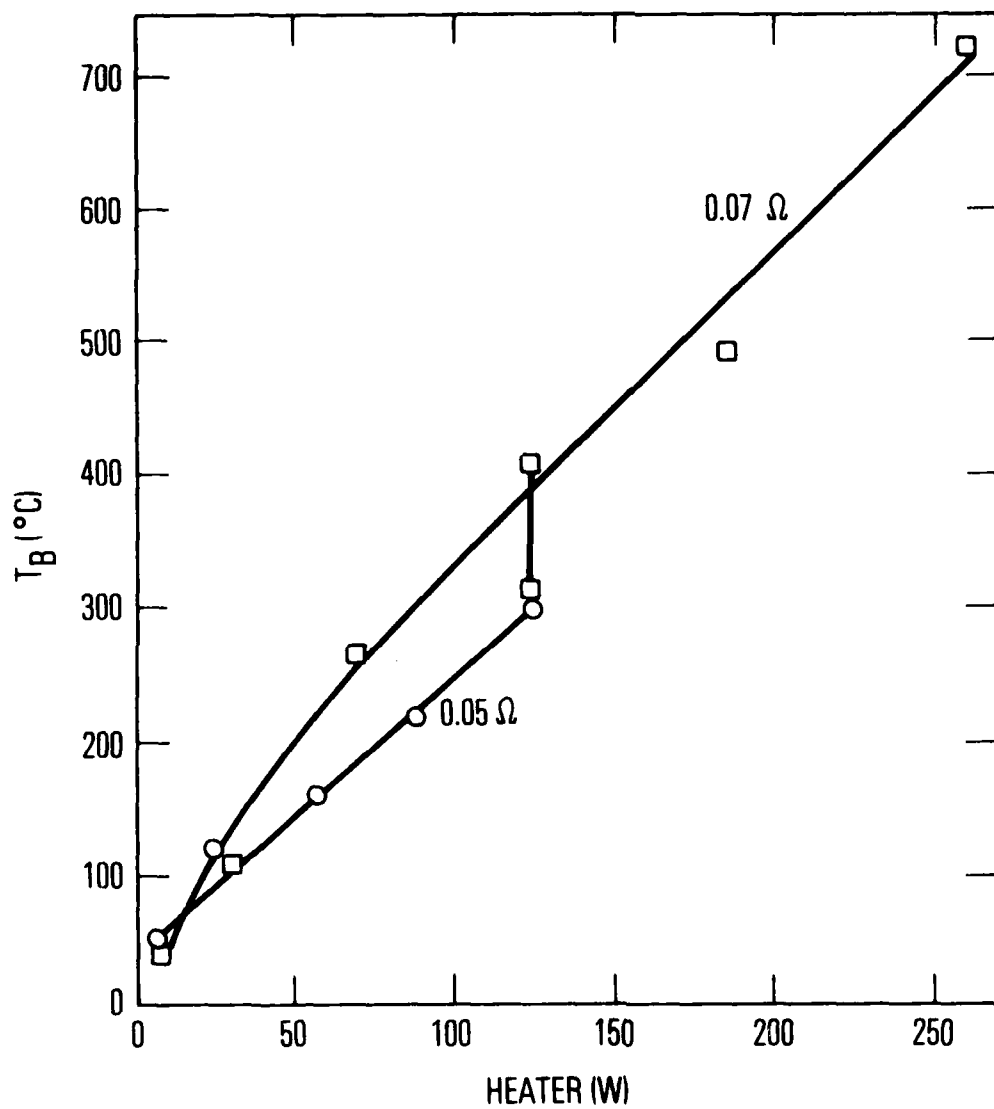


Fig. 2. Rise in Injector Temperature as a Function of Current Passed through Heater

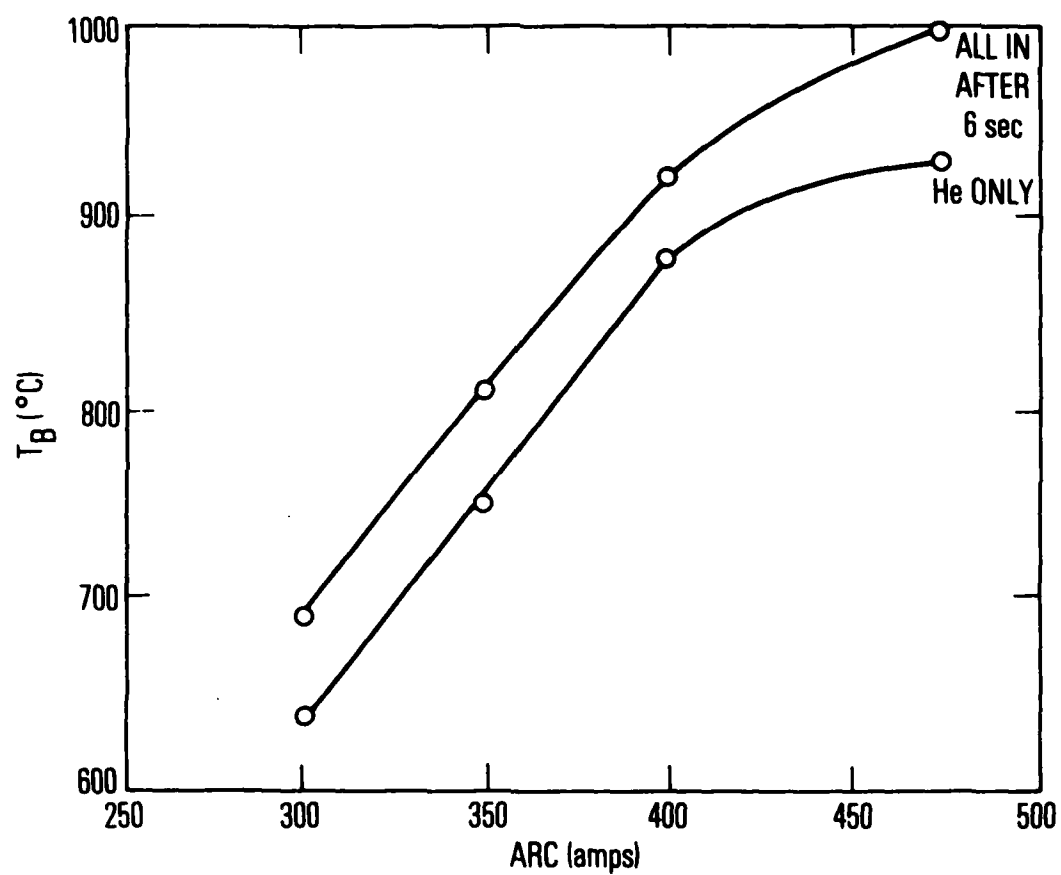


Fig. 3. Rise in Injector Temperature as a Function of Arc Current Used to Heat Plenum Gases

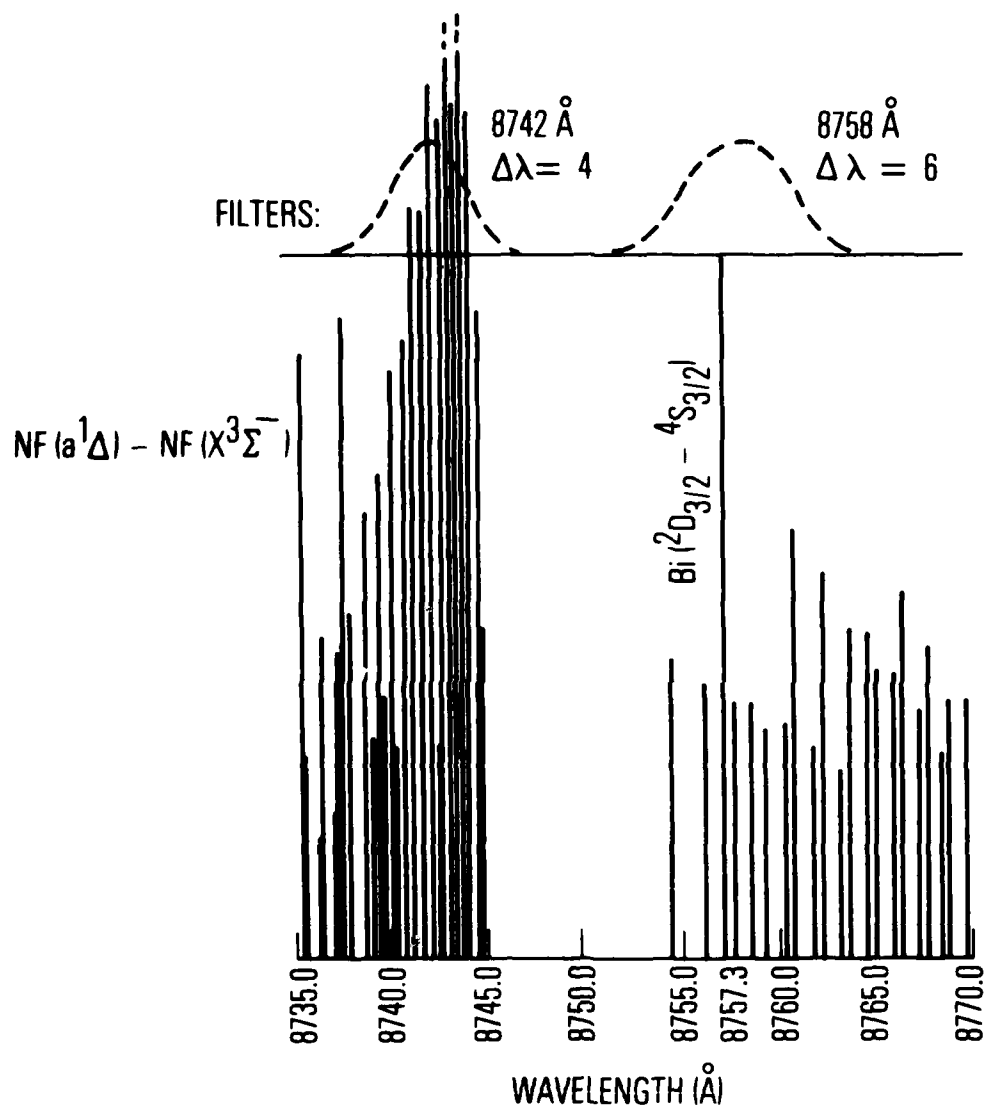
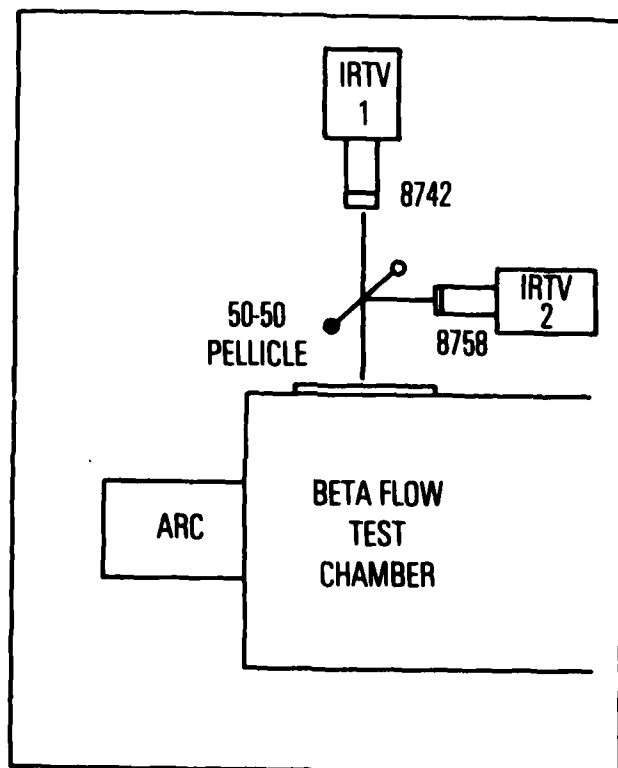


Fig. 4. Computed Line Spectra of Bismuth and NF Emissions, with Transmission Curves of the Two Narrow-Band Filters





**Fig. 5. Schematic of the Physical Arrangement of the Two Infrared-Sensitive Video Cameras with Respect to the Beta Flow Test Chamber**

### III. RESULTS AND DISCUSSION

The static pressure of the supersonic flow (solid lines), measured through a pressure tap located just above the metal injector in the wall of the upper shroud, is shown in Fig. 6. As expected, this pressure is sensitive to the flows of the constituent gases, in particular the  $N_2F_4$ . Test runs 517 and 518 are identical except for an increase in the arc current of 100 amps, from 350 to 450 amps. The significance of this increase is that it causes a corresponding increase in the temperature of the injector being heated by the flow (Fig. 7). From these measured temperatures and measured vapor-pressure curves of bismuth, as measured by Nesmeyanov<sup>13</sup>, the pressure of the bismuth inside the injector tube can be computed. The results of these calculations are shown in Fig. 6. For run 517 the bismuth vapor pressure is extremely low; therefore, very few bismuth atoms ever enter the gas stream. For run 518, however, the additional increase in temperature results in an order-of-magnitude increase in vapor pressure, which is comparable to the static pressure just as the  $N_2F_4$  is being turned off. (The  $N_2F_4$  valve is of a special design and takes several seconds to close, which thus provides a period over which the  $N_2F_4$  varies.) Decreasing the  $N_2F_4$  results in a corresponding drop in the static pressure, and for approximately 1.6 sec the pressure inside the injector exceeds the falling jet pressure. It is during this time, and this time only, that we observed chemiluminescence through the bismuth 8758-Å filter. No corresponding signal was observed by the camera with the 8742-Å filter, although the  $NF(a^1\Delta)$  emission was clearly discernible by both cameras.

The more recent work of Hultgren<sup>14</sup> indicates that the vapor pressures computed by Nesmeyanov,<sup>13</sup> as given in Fig. 8, are too high. Fortunately, lower values of the vapor pressure do not change the timing arguments but rather make them stronger. Moreover, we observed that when the metal injector was completely filled with metal, which removed all free volume, no anomalous 8758-Å emission was observed (as in run 518). This is consistent with the scenario that during the high-pressure portion of the run the helium and hydrogen enter the injector, and then, during the falling jet pressure (i.e.,

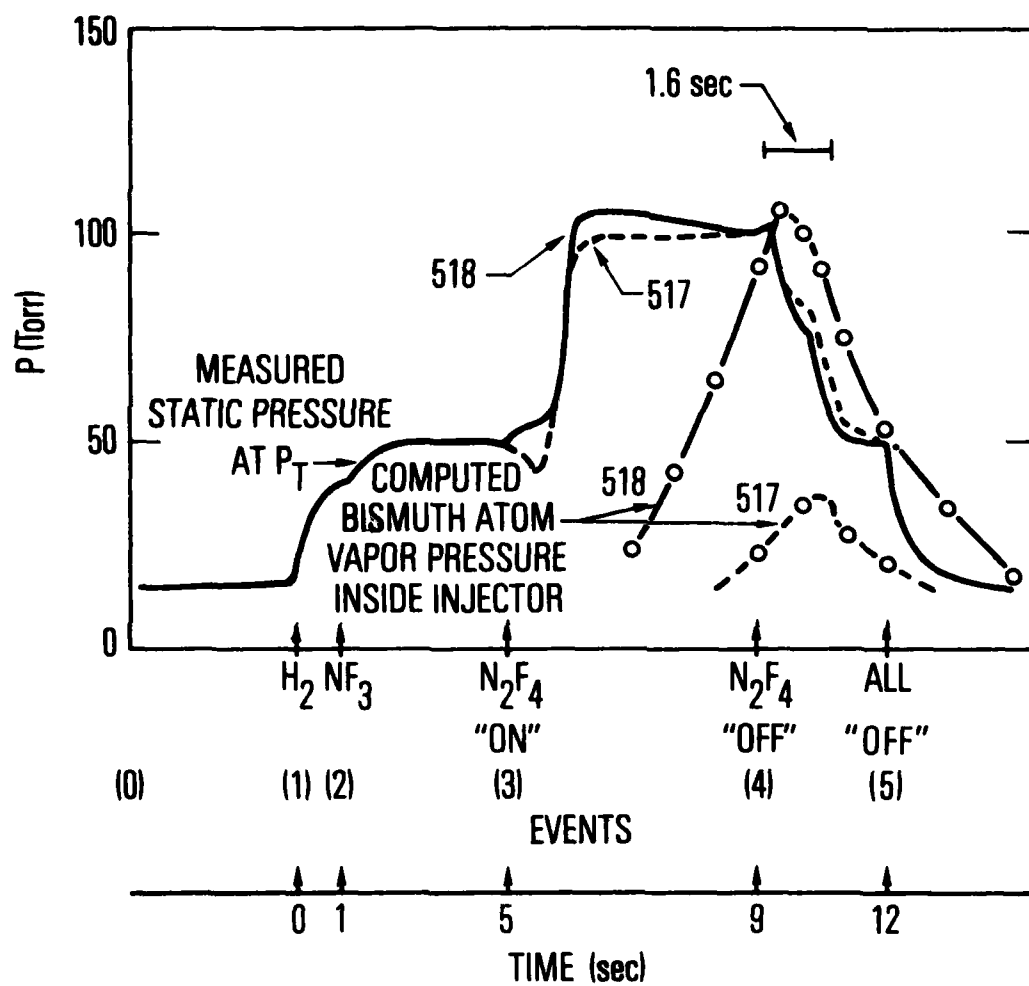


Fig. 6. Static Pressure of the Supersonic Flow and Computed Bismuth Atom Vapor Pressure inside Injector

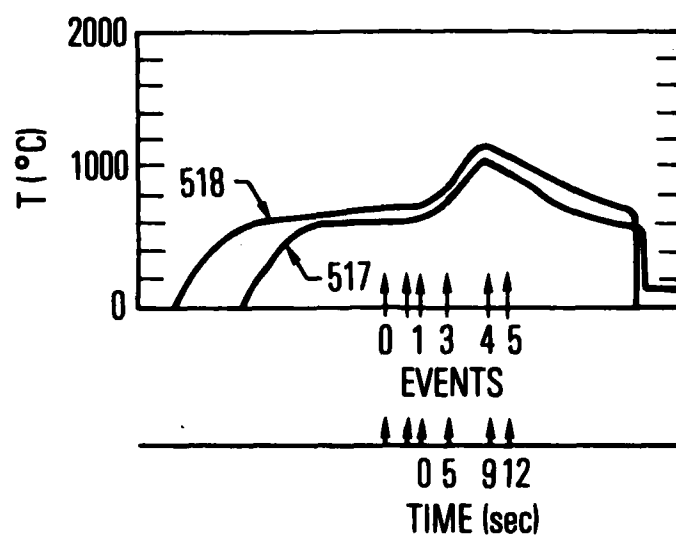


Fig. 7. Relationship of Injector Temperature to Increase in Arc Current with Time

for 1.6 sec), these gases, along with any bismuth atoms, escape. The relative amounts of bismuth atoms that escape are determined by the partial pressures, which are still an order of magnitude higher for run 518.

Figures 8a and 8b show the two-dimensional representation of the emission observed through the 8758-Å filter after being digitized by the Quantex. The flow is from left to right as in Fig. 1. The position and size of the injector and mounting bracket are indicated. The holes by which the bismuth vapor can be released into the flow are located on the top of the injector, as shown by the small arrow. Looking closely, one can see that the emission above the injector is greater in Fig. 8b (corresponding to run 518) than in Fig. 8a. This increased signal only persists for the 1.6 sec discussed above. Prior to this critical period, runs 517 and 518 are identical. Also indicated in Figs. 8a and 8b are the positions at which vertical and horizontal cross scales are taken. Figures 9a and 9b show these vertical scans for the upstream and downstream positions. The additional emission of run 518 on the downstream crosscut (V85) is clearly apparent over the corresponding emission of run 517. On the other hand, the upstream crosscuts are essentially the same. Similar remarks hold for Figs. 10a and 10b, which show the corresponding horizontal cross scans.

An analogous investigation of the emission signals recorded by the camera with the 8742-Å filter failed to show any correspondingly enhanced emission above the injector. Thus the enhanced emission is not caused by  $\text{NF}(a^1\Delta)$  and is localized in the 8758-Å spectral region, i.e., the region of  $\text{Bi}^*$  emission.

One can attempt to estimate the population density of the excited-state bismuth atoms relative to that of the  $\text{NF}(a^1\Delta)$  by comparing the signal levels of the two species, taking into account the number of lines and relative emission cross sections observed through the narrow-band 8758-Å filter (Fig. 5). This calculation involves the observation that, although there were 4 in. of holes in the injector, only the center inch showed appreciable mass loss; this suggests that the actual emission zone was only 1 in., or one-tenth the length over which the  $\text{NF}(a^1\Delta)$  emits radiation. Taking all these factors into account, we roughly estimate a relative bismuth atom density of approximately

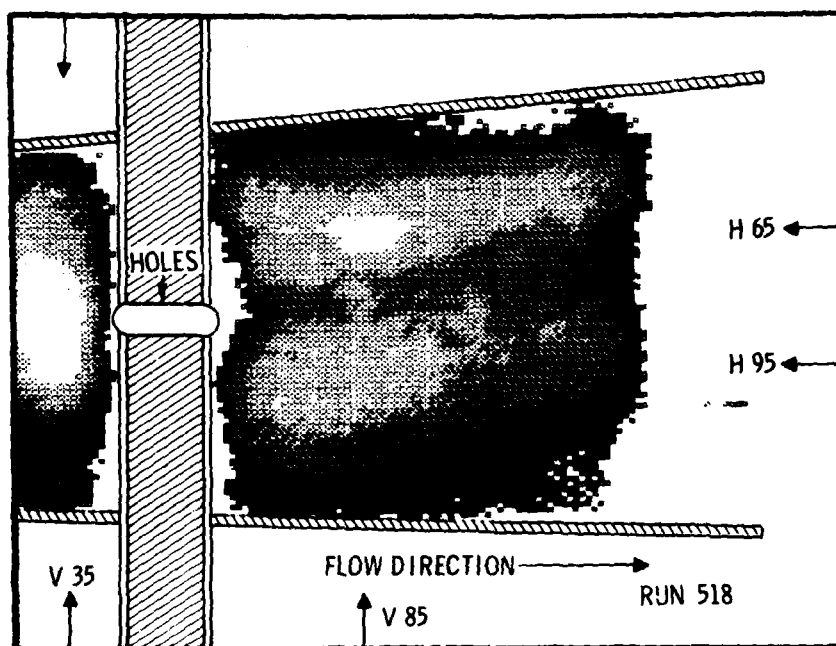
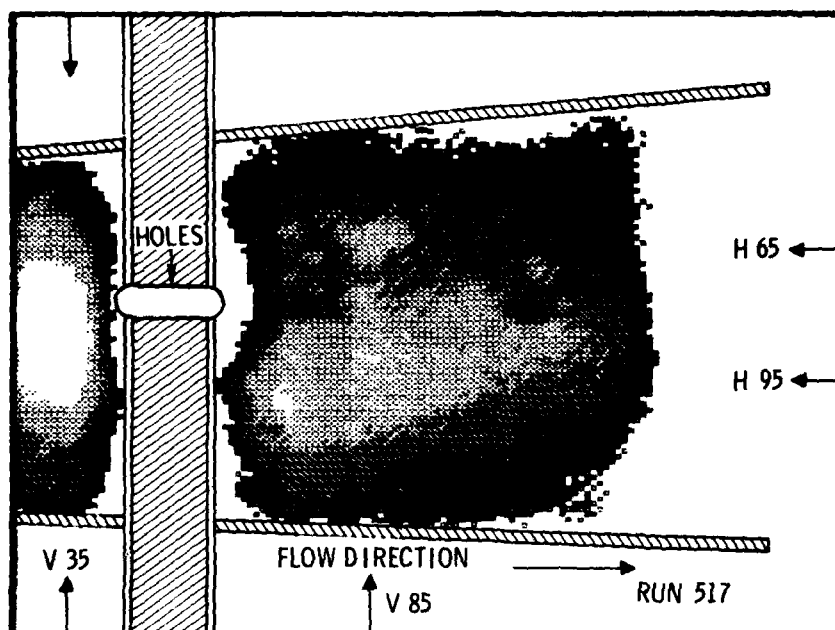


Fig. 8. Two-Dimensional Representations of the Emission Observed through the 8758-A Filter after Being Digitized by the Quantex

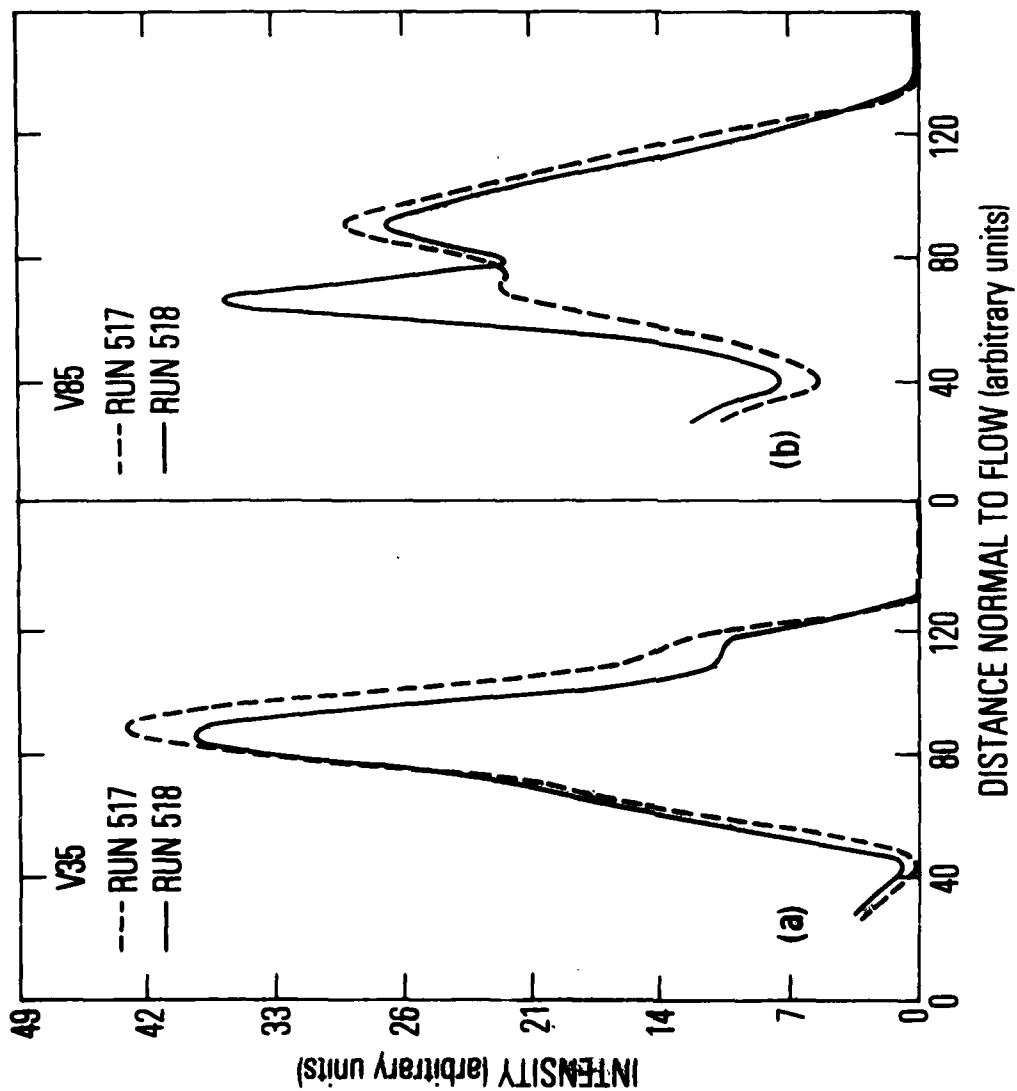


Fig. 9. Vertical Scans for Upstream and Downstream Cross Scale Positions Indicated in Fig. 8

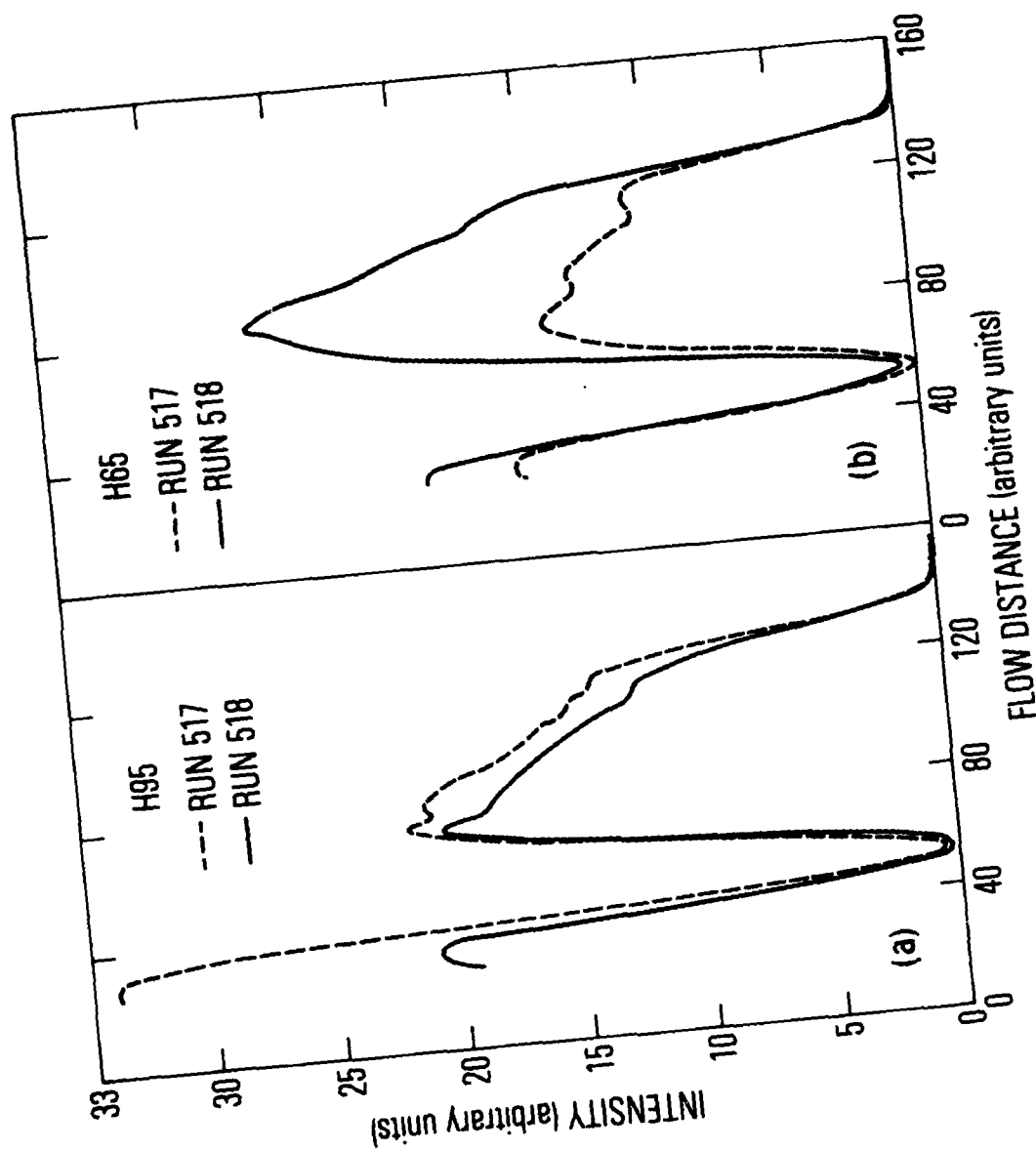


Fig. 10. Horizontal Scans for Upstream and Downstream Cross Scale Positions Indicated in Fig. 8



1% of the  $\text{NF}(a^1\Delta)$ . Although a rather low yield, this percentage represents a population density  $> 10^{13}$  atoms  $\text{cm}^{-3}$ , which is a scaling of several orders of magnitude over previous experiments. Perhaps of greater significance is the fact that the above calculation demonstrates that bismuth atoms can survive, at least for a few tens of microseconds, in the rather hostile environment of a reactive supersonic flow of  $\text{NF}(a^1\Delta)$ .

Unfortunately, because the bismuth atom vapor pressure is so sensitive to the flow conditions and because we rely on the flow itself to do the heating, the results were not as repeatable as we would have liked. As a consequence, this flow-heated metal injector approach has been discontinued in favor of the use of gaseous organo-bismuth compounds as a controllable source of atomic bismuth.

# REFERENCES

1. J. M. Herbelin and N. Cohen, Chem. Phys. Lett. 20, 603 (1973).
2. J. M. Herbelin, Chem. Phys. Lett. 42, 367 (1976).
3. C. T. Cheah, M. A. A. Clyne, and P. D. Whitefield, J. C. S. Faraday II 76, 711 (1980).
4. R. J. Malins and D. W. Setser, "Rate Constant and Branching Ratios, and Energy Disposal for NF(b,a,X) and HF(v) Formation from the H + NF<sub>2</sub> Reaction," J. Phys. Chem. 85, 1342 (1981).
5. J. M. Herbelin, D. J. Spencer, and M. A. Kwok, J. Appl. Phys. 48, 3052 (1977).
6. D. J. Miller, Advanced Laser Concepts, PR-77-2344 (U. S. Air Force Weapons Laboratory, 6 Jan. 1978), p. 110.
7. J. M. Herbelin, Development of an Efficient Supersonic Flow of Electronically Excited NF(a<sup>1</sup>Δ) Radicals, unpublished.
8. G. A. Capelle, D. G. Sutton, and J. I. Steinfeld, J. Chem. Phys. 69, 5140 (1978).
9. The σ is computed from the A coefficient reported by R. H. Garstang, J. Res. NBS 68A, 61 (1964).
10. "Experimental Transition Probabilities for Spectral Lines of Seventy Elements", NBS Monograph 53 (U.S. GPO, Washington, D.C., 1962), p. 562.
11. C. E. Moore, "Atomic Energy Levels," Circular of the NBS, Vol. III, 467, (U.S. GPO, Washington, D.C.1958), p. 245.
12. G. I. Segal, private communication [computed using wavelength data of W. E. Jones, Can. Journal of Phys. 45, 21, (1967)].
13. An. N. Nesmeyanov, Vapor Pressure of the Elements, trans. and ed. by J. I. Carasso (Academic, New York, 1963).
14. R. Hultgren, R. L. Orr, P. D. Anderson, and K. K. Kelley, Selected Values of Thermodynamic Properties of Metals and Alloys, Vol. I (Lawrence Radiation Laboratory, University of California, Berkeley, 1970).

#### LABORATORY OPERATIONS

The Laboratory Operations of The Aerospace Corporation is conducting experimental and theoretical investigations necessary for the evaluation and application of scientific advances to new military space systems. Versatility and flexibility have been developed to a high degree by the laboratory personnel in dealing with the many problems encountered in the nation's rapidly developing space systems. Expertise in the latest scientific developments is vital to the accomplishment of tasks related to these problems. The laboratories that contribute to this research are:

Aerophysics Laboratory: Launch vehicle and reentry aerodynamics and heat transfer, propulsion chemistry and fluid mechanics, structural mechanics, flight dynamics; high-temperature thermomechanics, gas kinetics and radiation; research in environmental chemistry and contamination; cw and pulsed chemical laser development including chemical kinetics, spectroscopy, optical resonators and beam pointing, atmospheric propagation, laser effects and countermeasures.

Chemistry and Physics Laboratory: Atmospheric chemical reactions, atmospheric optics, light scattering, state-specific chemical reactions and radiation transport in rocket plumes, applied laser spectroscopy, laser chemistry, battery electrochemistry, space vacuum and radiation effects on materials, lubrication and surface phenomena, thermionic emission, photosensitive materials and detectors, atomic frequency standards, and bioenvironmental research and monitoring.

Electronics Research Laboratory: Microelectronics, GaAs low-noise and power devices, semiconductor lasers, electromagnetic and optical propagation phenomena, quantum electronics, laser communications, lidar, and electro-optics; communication sciences, applied electronics, semiconductor crystal and device physics, radiometric imaging; millimeter-wave and microwave technology.

Information Sciences Research Office: Program verification, program translation, performance-sensitive system design, distributed architectures for spaceborne computers, fault-tolerant computer systems, artificial intelligence, and microelectronics applications.

Materials Sciences Laboratory: Development of new materials: metal matrix composites, polymers, and new forms of carbon; component failure analysis and reliability; fracture mechanics and stress corrosion; evaluation of materials in space environment; materials performance in space transportation systems; analysis of systems vulnerability and survivability in enemy-induced environments.

Space Sciences Laboratory: Atmospheric and ionospheric physics, radiation from the atmosphere, density and composition of the upper atmosphere, aurorae and airglow; magnetospheric physics, cosmic rays, generation and propagation of plasma waves in the magnetosphere; solar physics, infrared astronomy; the effects of nuclear explosions, magnetic storms, and solar activity on the earth's atmosphere, ionosphere, and magnetosphere; the effects of optical, electromagnetic, and particulate radiations in space on space systems.

END

DATE  
FILMED

11-82

DTIC